Appl. Phys. B 60, 543–552 (1995)

Applied Physics B Lasers and Optics

Transient grating optical nonlinearities in nematic, cholesteric and smectic liquid crystals

R. Macdonald, H. J. Eichler

Optisches Institut, Technische Universität Berlin, Strasse des 17. Juni 135, D-10623 Berlin, Germany
(Fax: +49-30/3142-6888)

Received: 31 March 1994/Accepted: 7 August 1994

Abstract. The transients of Kerr-like optical nonlinearities in various liquid crystals observed with picosecond light-induced dynamic gratings are discussed. It is shown that relatively high intensities and strong optical fields of short laser pulses lead to rapid molecular reorientation, ultrasound generation, multiphoton absorption, cholesteric helix deformation and other new phenomena which are not only of interest for basic liquid-crystal research but also determine photonic switching times in liquid crystalline all-optical devices.

PACS: 61.30.v; 42.65.k

The development of high intensity lasers and the discovery of materials with large optical nonlinearities in the last decades have extended the scope of nonlinear processes dramatically, resulting in considerable scientific and also practical interest [1]. Applications like phase-conjugation [2], photonic switching of light [3] or Second-Harmonic Generation (SHG) [4] are important aspects in modern laser physics and optical information technologies. Organic materials like liquid crystals and polymers presently receive strong attention [5] as promising candidates for nonlinear optical components because of large second- and third-order nonlinearities and the possibility to manufacture devices with large apertures in thin films of high optical quality. Furthermore, the optical and other physical properties can be varied widely in these materials by molecular engineering. The optical nonlinearities discussed in the following are describable by light-induced changes of the complex birefringence, i.e., changes in the refractive index or absorption for a given polarization, and therefore are called Kerr-like nonlinearities. Second-order processes like SHG which have also been investigated in poled or non-centrosymmetric liquid crytsals will not be treated here.

Light-induced changes of molecular orientation and alignment of liquid crystals have been studied as important mechanisms leading to rather strong but usually slow Kerr-like optical nonlinearities since the early 1980's. Typical response times with low power cw lasers range from submilliseconds up to seconds for these effects. General aspects and different details of optical nonlinearities in liquid crystals have been reviewed by several authors during the recent years [5–10].

It was realized later on [11] that the use of short intense laser pulses instead of low-power cw radiation may speed up the reorientational nonlinearity dramatically. Furthermore, a variety of different transient phenomena of liquid crystals can be investigated using short laser pulses. It was shown [11/13] that there is a transfer of energy, linear and angular momentum from the light wave to the liquid crystal during the impulsive excitation, which result in temperature rise, flow and reorientation of the molecules. Since these processes influence the optical properties of the material, the corresponding relaxation processes can be monitored with a weak probe beam. These advantages have been already pointed out in one of the first experiments using short laser pulses for the investigation of nematic liquid crystals reported by Hsiung et al. [11]. In this reference transient laser heating and optical reorientation in 5CB (*p*-pentyl-*p'*-cyanobiphenyl) was observed using Q-switched pulses of 6 ns duration. Photo-thermally induced birefringence changes [14, 15], optical reorientation [16], nonlinear absorption and refractive index changes (without reorientation) have been also investigated with nanosecond pulses in dynamic grating experiments or using the *z*-scan technique [17]. Some of the mechanisms and the complexity of processes leading to optically nonlinear behaviour in liquid crystals are schematically summarized in Fig. 1.

In order to achieve higher time-resolution it was demonstrated [18] that reorientation phenomena can be observed in nematic films even if subnanosecond pulses are used. In self-diffraction grating experiments with excitation pulses of 80 ps duration it was shown that molecular reorientation is mainly responsible for the diffraction effects. Time resolved picosecond grating experiments [12, 13, 18, 19] revealed, that these fast re-

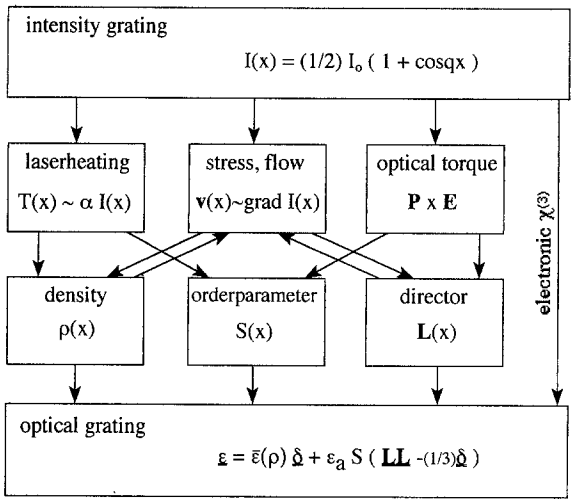

Fig. 1. Schematic representation of mechanisms leading to Kerr-like nonlinear optical behaviour in liquid crystals

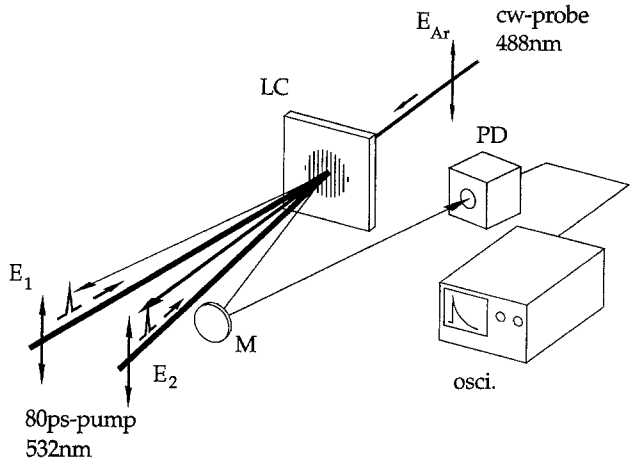

Fig. 2. Experimental arrangement for the investigation of light-induced dynamic gratings with *LC*, liquid crystal; *PD*, photodetector; *M*, mirror

orientation effects are followed by a rather complex dynamic response, because of coupling between density, temperature, flow and reorientation (Fig. 1). On the other hand, flow effects and density waves (ultrasound) can be excited much easier with picosecond than with nanosecond pulses.

In the following we review some of our recent results of time resolved investigations with picosecond laser pulses, which have been performed in nematic, smectic and cholesteric liquid crystals using the light-induced dynamic grating technique [20].

1 Experimental setup and results

The wave-mixing arrangement for the experiments is sketched in Fig. 2. Two pump-pulses of 80 ps FWHM at $\lambda_{exc} = 532$ nm obtained from a frequency-doubled mode-locked Nd:YAG laser with a symmetric beam splitter are slightly focussed to a spot size of about 500 μm diameter with an intersection angle of $\vartheta = 1$ deg onto the liquid-crystal sample. The two beams are linearly polarized, either parallel or perpendicular to each other. The optical fringes resulting from interference of the excitation beams modulate the optical properties of the liquid-crystal film due to optical nonlinearities. The fringe spacing is about $\Lambda = \lambda/\sin\vartheta = 30$ μm in the following.

The center of the induced optical grating is monitored by diffraction of a weak cw laser at $\lambda_{pr} = 488$ nm on a spot of 100 μm. The first-order diffracted intensity of the probe beam is measured as a function of time with the help of fast fotodetectors. In most experiments fast fotodiodes are used in connection with oscilloscopes and the temporal resolution is between 200 ps and 2 ns. Higher resolutions of several picoseconds are realized by using a streak-camera. The diffraction efficiency of a thin phase grating into the first-order diffracted beam is given by [20]

$$\frac{I_1}{I_0} = |\,J_1(\delta\varphi_0)\,|^2 \qquad (1)$$

where J_1 is the first-order Bessel function (of first kind) and $\delta\varphi_0 = 2\pi\delta n_0 d/\lambda$ denotes the amplitude of the induced phase grating for a given polarization of the probe beam. I_1 is the diffracted intensity of a probe beam with input intensity I_0. For weak gratings $\delta\varphi_0 \ll 1$ the approximation $J_1 = \delta\varphi_0/2$ holds and the diffracted intensity is proportional to the square of the induced refractive index changes.

It should be noted, that fast (subnanosecond) nonlinearities, which have been observed [18] in self-diffraction of the excitation beams are generally much weaker than the dynamic effects shown in the following and therefore do not appear in the transient grating signal obtained with the above described experimental technique.

1.1 Ultrasound generation. Flow-alignment and reorientation in nematics

Figure 3 displays oscilloscope traces of the diffracted probe-beam intensity on two different time scales obtained with a homeotropic aligend nematic film. An intensity grating (i.e., parallel polarized pump beams) of 80 ps duration has been used for the excitation. The initial molecular alignment is at a nonzero angle β with the intersection plane of the two pump beams to overcome the "nematic barrier" which usually occurs in reorientation phenomena at normal incidence.

Obviously, the dynamic response of liquid crystals to short intense laser pulses is rather complex, showing several characteristic relaxation processes and time constants. The grating is built-up on a nanosecond time scale and the diffracted signal is still increasing long after the pump pulse has left the sample. Afterwards the grating washes out and the diffracted signal decays with a double exponential law with two time constants of about 200 μs and 40 ms, respectively. The slow relaxation process can be attributed to collective molecular reorientation effects whereas the faster process is the decay of thermal gratings due to heat diffusion. The observed slow relaxation times

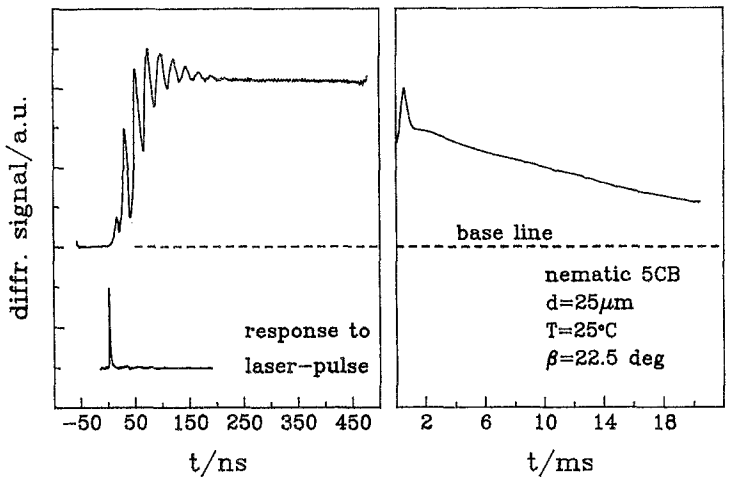

Fig. 3. Diffracted probe-beam intensity vs. time after ps grating excitation with parallel polarized pump-beams for a slanted homeotropic nematic sample. The angle between the polarization and the initial alignment is denoted as β. Excitation energy is $W_p = 0.25$ mJ

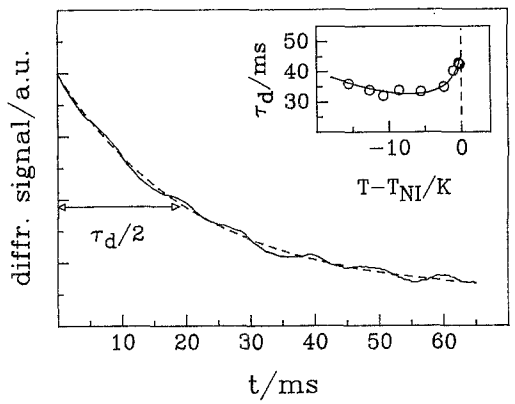

Fig. 4. Reorientation grating decay after excitation with 80 ps laser pulse. *Inset:* Evaluated relaxation times vs. reduced temperature. $T_{NI} = 36.5°$ C is the nematicisotropic phase transition temperature

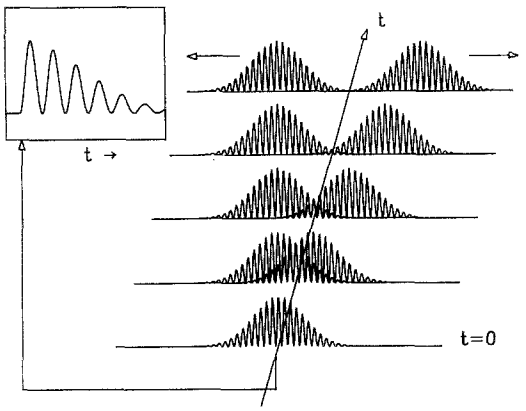

Fig. 5. Schematic representation of holographic ultrasound generation: Two sound wave packets are launched by spatially periodic squeezing and stretching of the liquid crystal with an intensity grating at $t = 0$

exhibit a characteristic temperature dependence shown in Fig. 4 which has been explained [13] with the temperature dependences of the rotational viscosity γ_1 and the elastic constant K [24] of the liquid crystal, confirming that reorientation has been induced with picosecond laser pulses. The thermal grating relaxation is treated in Sect. 1.2 with more detail.

The strong oscillations during the grating build up are due to laser-induced standing ultrasound waves [21, 22] and diffraction at the resulting density modulations ("forced Brillouin scattering"). The holographic generation of ultrasound is explained schematically in Fig. 5. A density modulation with the spatial frequency q of the intensity grating is excited at $t = 0$ by thermal volume expansion or electrostrictive forces. The periodic stretching and squeezing of the fluid within the excitation area launches two counterpropagating sound wave packets if the corresponding frequency

$$\omega = c_s q \tag{2}$$

is included within the Fourier spectrum of the excitation pulse. c_s is the speed of sound. As a result, the density modulation and the corresponding phase grating relax in form of a damped standing wave leading to oscillations in the diffracted signal ("acoustic ringing").

The numerical value of the frequency given by (2) for $q = (2\pi/30\ \mu\text{m})$ and $c_s = 1500$ m/s from [22] is $\omega/2\pi = 50$ MHz in agreement with the oscillations in Fig. 3. The holographic sound wave generation is very effective if the pulse duration $\tau_p \ll \omega^{-1}$.

The damping of the acoustic grating signal is given by two mechanisms in general. First, the kinematic viscosity η of the fluid leads to a phonon life-time [23]

$$\tau_1 = 2/(\eta q^2)\,. \tag{3}$$

Second, the two sound wave packets travel out of the excitation region leading to effective damping of the signal which can be calculated to

$$\tau_2 = w_0/c_s \tag{4}$$

where w_0 is the excitation beam radius. The phonon life-time can be observed only if $w_0 \gg 2\, c_s/(\eta q^2)$. The damping of the signal displayed in Fig. 3 is mainly given by the second process described by (4).

The observed acoustic gratings are a new quality appearing in transient grating experiments with picosecond laser pulses since they are connected with translational motions of the liquid-crystal molecules, which can be neglected in most experiments with cw lasers. In liquid crystals translational motions are usually coupled to rotation and reorientation of the molecules via anisotropic frictional forces. Shear-induced flow-alignment of liquid-crystal films between two moving glass-plates [24] is a well-known example for this phenomenon. The importance of flow-alignment effects in *ps* grating experiments has been demonstrated by Khoo et al. [12] and by us [13, 19] almost simultaneously. In [12] reorientation effects due to temperature and density modulations have been observed in an experimental arrangement where *parallel* polarizations of the excitation beams nearly normally incident on a homeotropic liquid crystal did *not allow* optical torque-induced reorientation in principle. In [13, 19] investigations have been performed with a different geometry which *allows* laser-induced reorientation effects, on one hand, but uses *crossed* excitation beam polarizations to avoid thermal and acoustic gratings, on the other hand. It was shown that the excitation pulse is followed by a delayed reorientation process in this case, which can be explained in terms of a large "inertial moment" due to flow-alignment, which is not driven by temperature and density modulations but by photoelastic stresses.

Thermal gratings and the resulting acoustic gratings can be suppressed if crossed polarizations $E_1 \perp E_2$ of the pump beams are used with moderate excitation energies (below 0.6 mJ in our experiments) instead of parallel polarizations $E_1 \parallel E_2$. The resulting diffraction signals are shown Fig. 6. If $E_1 \parallel E_2$ the two beams interfere to give an intensity grating while for $E_1 \perp E_2$ a polarization grating with a much weaker intensity modulation (due to imperfect polarizations of the beams) is formed. As a consequence, polarization-dependent effects like reorientation are excited with crossed polarizations while intensity-dependent modulations like thermal gratings are suppressed at the same time. Furthermore shear forces and transverse flow effects can be excited with polarization gratings, which result from photoelastic stresses [23].

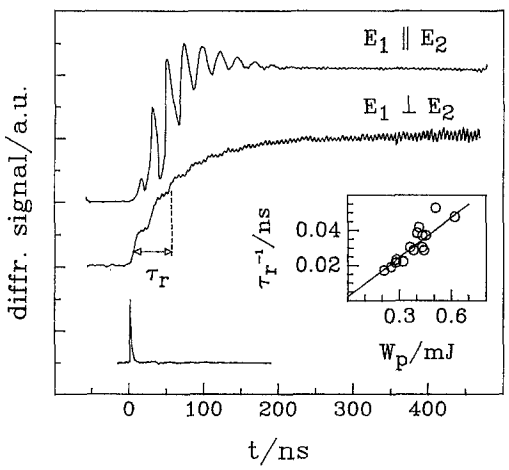

Fig. 6. Diffracted probe-beam signal vs. time with parallel and crossed pump-beam polarizations. Excitation energy is $W_p = 0.25$ mJ

Since the elasto-optic coefficients relating these stresses to the light field are not known for liquid crystals, the force density **F** corresponding to Maxwell stresses [25]

$$\mathbf{F} = (\mathbf{D} \cdot \nabla)\, \mathbf{E}^* - \frac{1}{2} \nabla (\mathbf{E} \cdot \mathbf{D}^*) \tag{5}$$

can be used as a qualitative approximation. **E** is the optical field, **D** is the displacement vector, and the asterik denotes the complex conjugate. The complex notation gives the time-averaged real value of **F**. The main force for a polarization grating with an experimental geometry as depicted in Fig. 2 is given by the x-component $F_x = \frac{1}{2} \varepsilon_0\, \varepsilon_\perp\, n_\perp\, q E^2 \cos(qy)$ and other components are negligible. The director motion can be described by a single reorientation angle Θ in this case, which is obtained by a torque balance in addition to the Navier-Stokes equation [26, 27]

$$\gamma_1\, \partial_t \Theta + M_{el} + M_f + M_{0p} = 0\,, \tag{6a}$$

$$\varrho\, \partial_t v_x - \gamma_s \Delta v_x = F_x, \tag{6b}$$

where $\partial_t = \partial/\partial t$, $M_{el} = -K \Delta \Theta$ is the elastic torque, $M_f = -\frac{1}{2}(\gamma_1 - \gamma_2 \cos 2\Theta)\, \partial v_x/\partial z$ is a flow coupling term and $M_{0p} = -\frac{1}{2} \varepsilon_0 \varepsilon_a E^2 \sin[2(\beta + \Theta)]$ is the optical torque. γ_s and γ_2 are flow viscosities, ϱ is the mass density and v_x the flow velocity excited by F_x. The inertial moment (density) connected with pure reorientation phenomena (i.e., no flow) is in the order of $\mu = 10^{-16}$ kg/m and has been ommited from (6a) because it would result in reorientation rise time of picoseconds or less, which was not observed in these experiments. The inverse flow alignment process has been also estimated to be of less importance and is neglected here.

We will not discuss the solution of (6) here in much detail but briefly summarize the main results as given in [13]: A single equation describing the time dependence of the reorientation grating amplitude in terms of an overdamped oscillator can be obtained by elimination of the flow velocity. The apparent second time derivative in this equation is a consequence of the flow elimination and is connected with a large inertial moment $\tilde{\mu} \approx \varrho/q\, q'$ of the flowing molecules in the excited regions, where q is the wave number of the excited transverse and $q' = 2\pi/d$ the longitudinal spatial mode. It can be calculated to $\tilde{\mu} = 10^{-8}$ kg/m which is much larger than the inertial moment given above and consequently leads to much slower reorientation rise times. The dynamics of the reorientation grating amplitude according to eqns. 6 for

excitation with a delta pulse is then given by

$$\Theta_1 \sim [\exp(-t/\tau_d) - \exp(-t/\tau_r)] \tag{7}$$

where $\tau_r = \varrho/\gamma_s(q^2+q^2)$ and $\tau_d = \gamma_1/K(q^2+q^2)$ can be interpreted as the rise time and the decay time of the reorientation process.

As with simple reorientation models, the relaxation of the grating is given by the rotational viscosity and the elastic constant of the nematic fluid, whereas the observed rise times are governed by the damping of the induced shear flow and hence the flow viscosity. The observed rise times τ_r are in the order of 20 to 50 ns depending on pump energy (Fig. 6). The energy dependence can be explained assuming a non-Newtonian flow viscosity, which means that the viscosity and thus τ_r^{-1} contains a term which is proportional to the shear rate $\partial v_x/\partial z$. Since v_x is proportional to the pump energy W_p, see (5, 6), a linear dependence of the inverse rise time on pump energy can be expected, in agreement with the experimental observations (Fig. 6). By extrapolating the graph to $W_p \to 0$ and using τ_r as given with (7) we obtain $\gamma_s = 0.02$ kg/ms in excellent agreement with published data for small shear rates [28].

It should be noted at the end of this section that longitudinally translational motion of molecules and ultrasound has been also observed even with polarization gratings at higher excitation energies [18]. This may result from imperfect polarizations of the excitation beams and/or depolarization effects inside the liquid crystal film, both resulting in additional intensity modulations at stronger excitations.

1.2 Nonlinear absorption and thermal gratings

Besides the "giant" reorientational nonlinearity, laser-induced thermal birefringence changes in slightly absorbing nematic liquid crystals have been investigated as important optical nonlinear mechanisms in various experiments [11, 14–16] using short laser pulses. The observed large thermo-optic effects are, however, not explainable by the rather weak linear absorption of the most stable and technically important family of liquid crystals, the cyanobiphenyls, throughout the whole visible and near infrared spectral range as mentioned above. As a consequence, the absorption of these transparent materials has been usually enhanced by adding appropriate dyes or by coating the inner walls of the liquid crystal cell with absorbing layers [29, 30] to obtain strong laser heating and the related thermal nonlinearity.

However, enhanced absorption and thermal gratings *without* any additional absorbing material has been also observed in 5CB using short intense laser pulses in the green spectral range, recently. Deeg and Fayer [31] observed two-photon absorption (2PA) and excited state gratings in wave-mixing experiments with 300 fs laser pulses in isotropic 5CB at $\lambda_{exc} = 575$ nm. We verified experimentally [32] that strong thermal gratings in the nematic and the isotropic phase of 5CB are generated by a three-photon process if short picosecond laser pulses at $\lambda_{exc} = 532$ nm are used. The heat production was explained to result from radiationless recombination of highly excited states, which are populated by 2PA and subsequent excited state absorption as will be shown below. Nonlinear absorption in 5CB has been also observed [17] using nanosecond pulses in the green spectral range during z-scan measurements.

The experiments discussed in the following have been performed in our transient grating arrangement using a planarly aligned nematic sample and $\beta = 0$. The polarizations ($E_1 \parallel E_2$) of the pump beams, the grating wave vector and the normal axis of the liquid crystal film are orthogonal to each other and may be labelled as the x-, y- and z-coordinate axis, respectively. The sample can be rotated around the z-axis to orient the optical field either parallel or perpendicular to the nematic director. This is important to avoid strong additional reorientation gratings as discussed in the previous subsection.

The absorbed intensity grating modulates the temperature and hence the birefringence of the fluid leading to diffraction of the probe beam. The temperature rise δT due to laser heating can be described by the heat flow equation [20]. Solution of this equation in a plane wave approximation neglecting higher Fourier-components of the grating may be written as [32]

$$\delta T = T - T_0 = \frac{Q_0 \tau_p}{ec} \exp(-t/\tau)(\cos(qy)) \tag{8}$$

where the thermal grating relaxation time $\tau = D_{\text{eff}}^{-1} q^{-2}$ contains the relevant (effective) heat diffusion coefficient and the grating wave number $q = 2\pi/\Lambda$. The heat production (per time and volume) referring to the amplitude (peaks) of the induced grating is denoted as Q_0, τ_p is the laser pulse duration, ϱ the mass density, c the heat capacity and T_0 is the initial temperature. In evaluating (8) we have assumed that the heat production is fast compared to the thermal relaxation times and that the main heat diffusion washing out the grating is from the peaks to the nulls of the grating.

Heat diffusion in nematic liquid crystals is governed by a second-rank tensor $\mathbf{D} = \lambda_w \varrho^{-1} c^{-1}$ which is given by the heat conductivity tensor λ_w, the mass density ϱ and heat capacity c. The effective heat diffusion coefficient D_{eff} is, e.g., given by the two principal values $D_\perp$ and $D_\parallel$ in the nematic phase if the temperature gradient (i.e., the grating wave vector) is applied perpendicular or parallel to the planar aligned director, respectively. Typical values for D_{eff} and τ are dicussed below, together with the experimental results.

The heat production in the sample and thus the amplitude of the induced thermal grating at the beginning of the decay is determined by the absorbed intensity of the ps-excitation pulse. In many cases it is sufficient to use expressions [7,20] like $Q = \alpha I$ where α is the absorption coefficient and I the intensity, which implies, however, that the absorbed intensity is fast and completely dissipated as heat. According to [31] strong two-photon absorption (2PA) from the lowest energy band S_0 to the first excited singlet states S_1 can be expected in experiments with intense green laser pulses at $\lambda_{exc} = 532$ nm.

The 2PA spectra essentially follows the one-photon absorption which peaks at $\lambda = 280$ nm in pure 5CB [5]. The 2PA probability is proportional to the number density of ground state molecules and the photon density, i.e., the intensity. The absorption coefficient can be written in this case as $\alpha_{2PA} = \gamma_2 I$, where γ_2 is a constant. However, since the lifetime of the S_1-state is in the order of one nanosecond or somewhat less [33], there is a strong probability that a third photon of the short picosecond laser pulse is absorbed by an excited state-excited state transition $S_1 \rightarrow S_2$. The one-photon excited-state absorption is very effective if the excitation pulse duration is short compared to the S_1 lifetime, but large compared to the solvent cage reorganization time of 4 ps. The latter is important because the transition is shifted down to the excitation wavelength $\lambda_{exc} = 532$ nm by this process [31]. A spectroscopic investigation of the excited state absorption in 5CB is reported in [34].

The probability for the one-photon excited state absorption is proportional to the number density of singlet S_1 molecules which is proportional to the intensity absorbed by 2PA in our case, i.e. $\alpha_{12} = k\alpha_{2PA} I = \gamma_3 I^2$ where $\gamma_3 = k\gamma_2$ and k is a constant. The complete three-photon absorption process can then be described by the nonlinear absorption coefficient

$$\alpha = \alpha_{2PA} + \alpha_{12} = \gamma_2 I + \gamma_3 I^2 = \gamma_2 I(1 + kI) . \quad (9)$$

The intensity independent $S_0 - S_1$ one-photon absorption has been neglected because it is rather weak for our excitation wavelength, as discussed above.

The heat production due to this nonlinear absorption is provided by fast radiationless recombination from the S_2 singlet states mainly and can be written as

$$Q = \alpha_{12} I = \gamma_3 I^3 . \quad (10)$$

The temperature rise and the amplitude of the induced thermal grating can be calculated by using (8 and 10). As a result, the induced phase grating amplitude $\delta\varphi_0$ is expected to be proportional to I^3 or W_p^3, respectively, because $\delta n \sim \delta T$. In Fig. 7 we have plotted $\delta\varphi_0$ as a function of the excitation energy on a logarithmic scale, which has been obtained from diffraction efficiency measurements, using (1), with isotropic 5CB displayed in the inset of the same figure. The experimental data fit quite well to a cubic law which is a strong indication that the three-photon absorption process is mainly responsible for the heat production. Laser heating due to 2PA or one-photon absorption would result in a quadradic or linear dependency, respectively.

The coefficients γ_3 have been evaluated from these experiments to $\bar{\gamma}_3 = 3.7 \cdot 10^{-25}$ m^3/W^2 in the isotropic phase and $(\gamma_3)_\perp = 0.14\,\bar{\gamma}_3$, $(\gamma_3)_\parallel = 1.8\,\bar{\gamma}_3$ in the nematic phase at $T = 25°$ C. The nonlinear absorption is anisotropic in the nematic phase with stronger absorption for polarizations parallel to the director. This is not surprising since the involved $S_0 - S_1$ transition is polarized along the long molecular axis in cyanobiphenyls.

Intensity dependent absorption, of course, leads to nonlinear transmission of the samples, which has been clearly observed [32] with liquid crystal films of 200 μm thickness.

Relaxation of the picosecond induced thermal gratings ranges on a microsecond time scale and exhibits a critical slowing behaviour in the vicinity of the nematic-isotropic phase transition. Figure 8 shows the evaluated thermal relaxation times which depend on director orientation and temperature. The two branches for τ in the nematic phase correspond to heat diffusion parallel and perpendicular to the director. Typical values for the relaxation times not too close to the phase transition (e.g., at $|T - T_{NI}| = 10$ K) are $\tau_\perp = 250$ μs, $\tau_\parallel = 130$ μs and $\tau_{iso} = 180$ μs which can be explained with the thermal relaxation time in (8) using $q = 0.2\ \mu\text{m}^{-1}$ and heat diffusities like $D_\perp = 0.9 \cdot 10^{-3}\ \text{s}^{-1}\,\text{cm}^2$, $D_\parallel = 1.8 \cdot 10^{-3}\ \text{s}^{-1}\,\text{cm}^2$ and $D_{iso} = 1.3 \cdot 10^{-3}\ \text{s}^{-1}\,\text{cm}^2$ in good agreement with published data [7].

The observed temperature dependence of τ can be explained mainly with the temperature dependence of the heat conductivity tensor and the heat capacity c at the first-order nematic-isotropic phase transition [32].

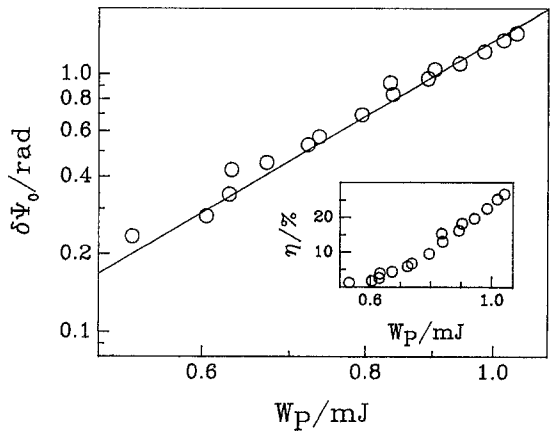

Fig. 7. Evaluated thermal grating modulation depth vs. excitation energy for isotropic 5CB. The *inset* shows the measured diffraction efficiencies

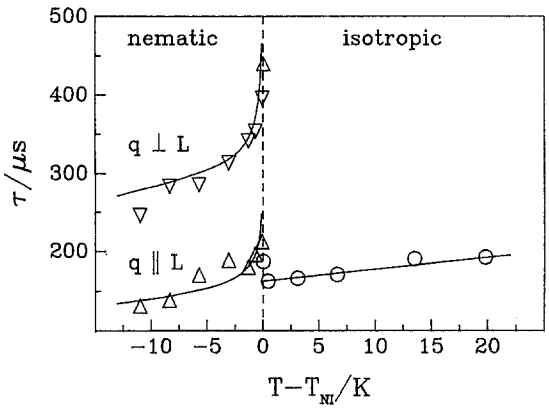

Fig. 8. Thermal grating relaxation times and anisotropic heat diffusion in 5CB as a function of temperature. T_{NI} is the nematic-isotropic phase transition temperature

1.3 Photo-thermal reorientation of ferroelectric liquid crystals

Recently, a new optically induced reorientation effect has been proposed and demonstrated [30] using ferroelectric liquid crystals. Photo-thermally induced optical axis reorientation of 23 deg was used to realize an optically adressed half-wave plate and all-optical modulation with low-power cw lasers. The dynamics of these reorientation effects have been also investigated using short picosecond laser pulses and the transient grating technique [35]. Due to a rather fast temperature rise induced by impulsive laser heating it is possible to investigate the relaxation of the tilt angle towards the new equilibrium state. This relaxation process is not only of practical interest for the realization of optical switching times but also for fundamental research, since the tilt angle can be used as an order parameter [36] to describe the SmC* – SmA phase transition.

The experiments have been performed with surface stabilized smectic films in a bookshelf-like geometry (Fig. 9). The director and hence the optical axis is tilted with respect to the smectic layers including an angle Θ. The tilt angle is temperature dependent, as depicted in Fig. 10. Due to residual absorption of the laser pulse within the sample the temperature is increased rapidly and the tilt angle follows with the so-called soft-mode relaxation time. A nonlinear dynamic equation describing this reorientation process can be written using a Landau-type potential for the stationary description of the SmC* – SmA phase transition as

$$\gamma \partial_t \Theta + A_0 (T - T_c)\, \Theta + B \Theta^3 = 0 \qquad (11)$$

where γ is a viscosity, T_c the phase transition temperature and A_0, B are constants. Eq. (11) can be solved assuming small light-induced pertubations in the temperature $T = T_{eq} + \bar{T}$ and the tilt angle $\Theta = \Theta_{eq} + \bar{\Theta}$ and neglecting all higher than linear terms in these pertubations to give

$$\bar{\Theta} = \bar{\Theta}_0 [\exp(-t/\tau_w) - \exp(-t/\tau)] \qquad (12)$$

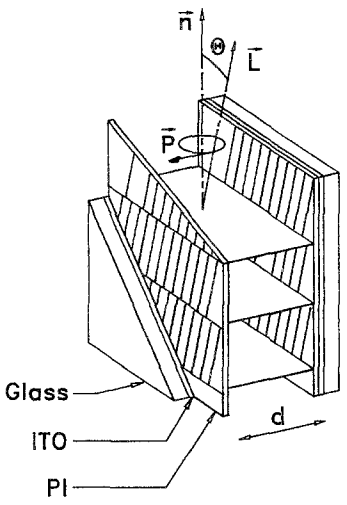

Fig. 9. Surface stabilized SmC* ferroelectric liquid crystal in a bookshelf-life geometry, with **L**, director; **n**, layer normal axis; **P**, spontaneous polarization; Θ, tilt angle; $d = 2\ \mu m$

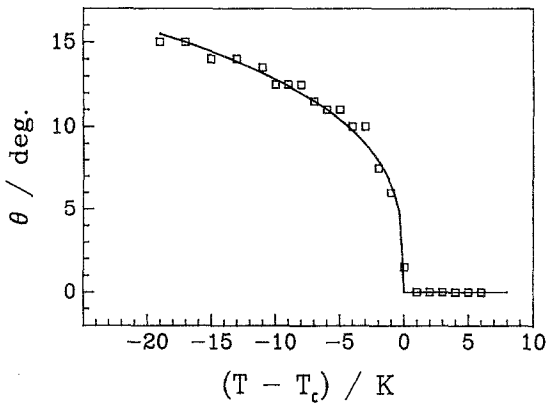

Fig. 10. Tilt angle of ferroelectric ZLI 4237-100 (Merck) vs. temperature. T_c is the SmA–SmC* phase transition temperature

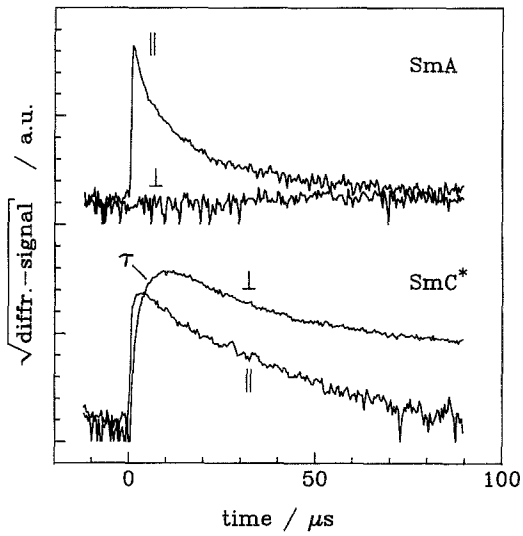

Fig. 11. Square root of the diffracted signal vs. time for the SmC* and SmA phase of a ferroelectric liquid crystal

where $\tau = \gamma [2 A_0 (T_c - T_{eq})]^{-1}$ is the soft-mode relaxation time (for $T_{eq} < T_c$) and τ_w the thermal relaxation time, assuming $\bar{T} = \bar{T}_0 \exp(-t/\tau_w)$. The soft-mode relaxation described by (12) leads to a delayed increase of the diffracted probe beam as can be seen in Fig. 11. Experimental results obtained within the SmC* and SmA phase are shown for comparision. Since the birefringence and film thickness are matched to provide that $n_a d \approx \lambda/2$, periodic reorientation of the optical axis leads to a strong depolarization of the diffracted probe beam. This has been investigated by performing a polarization analysis of the diffracted light. The orthogonally polarized signal is much stronger in the SmC* phase, indicating optical axis reorientation, whereas no depolarization effects occur in the SmA phase. The grating diffraction in the SmA phase is explained by density modulations mainly and no reorientation has been observed. The density relaxation is, however, not connected with acoustic gratings in contrast to the considerations of Sect. 1.1 since the liquid crystal film is rather thin resulting in strong damping of sound waves.

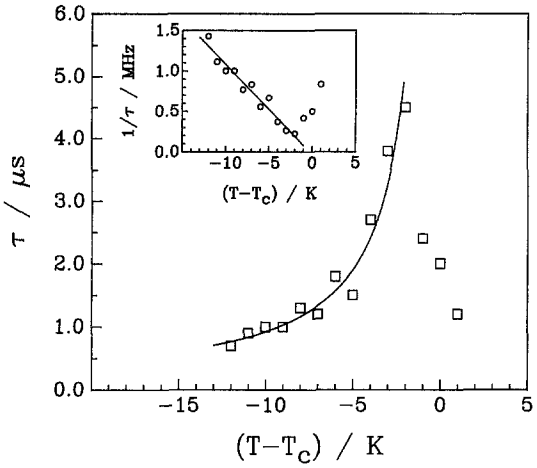

Fig. 12. Temperature dependence of the evaluated soft-mode relaxation times. T_c is the SmA–SmC* phase transition temperature. The *inset* shows the reciprocal relaxation times vs. temperature

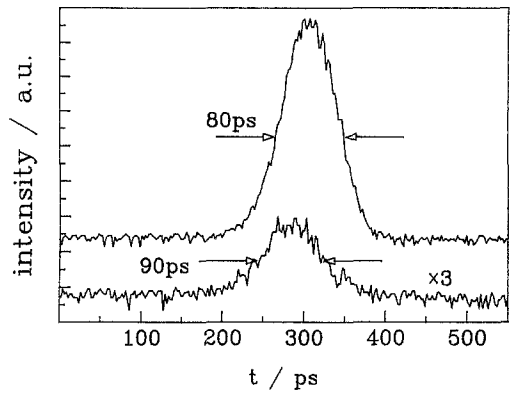

Fig. 13. Temporal development of selfdiffracted intensity into first diffraction order (*lower trace*) compared with input laser pulse (*upper trace*). The vertical scale of the diffracted intensity has been expanded by a factor 3 with respect to the incident intensity

The observed order parameter relaxation times are in the range of 0.6 to 5 μs with the commercial ferroelectric liquid crystal ZLI 4237-100 (supplied by Merck), depending on temperature, as shown in Fig. 12. The hyperbolic increase of τ with increasing temperature can be expected from the dynamic model of the phase transition discussed above.

The grating decays on a microsecond time scale if low excitation energies (≤ 100 μJ) are used. Relaxation of the thermal gratings in this case is determined by surface heat diffusion because the liquid crystal is rather thin compared with the grating period. The nonexponential decay as shown in Fig. 11 is about one order of magnitude faster than for thicker films (Fig. 8) which can be explained [37] by solving the heat diffusion equation for this particular case.

If, however, the excitation is stronger (> 100 μJ), a slower component can be observed following the thermal relaxation. The time constants of the slow component are in the range of several milliseconds and can be explained by the relaxation of elastic deformations. Strong distortions of the smectic layers may further lead to permanent gratings which has been also reported by Khoo et al. [12]. These permanent gratings can be erased by carefully heating and subsequent cooling of the whole sample. Eraseable permanent gratings are important, e.g., in applications like holografic optical data storages.

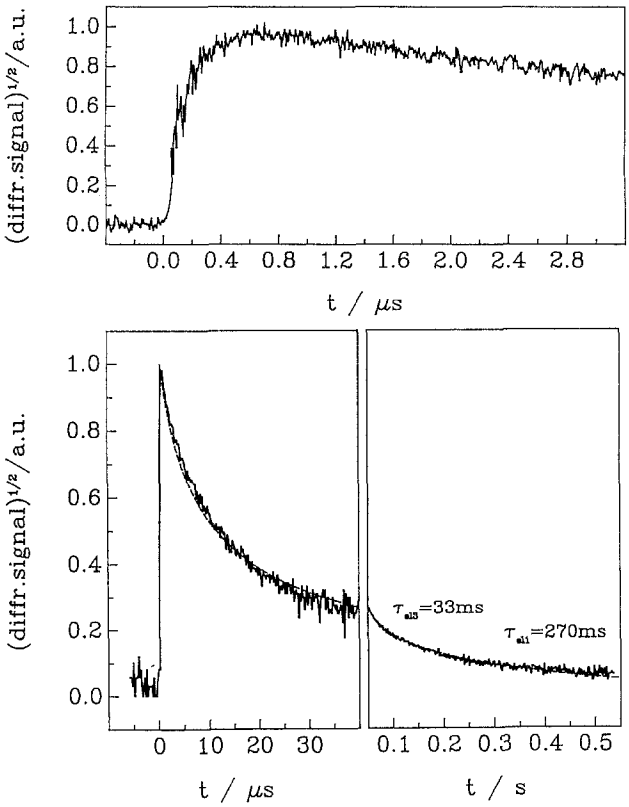

Fig. 14. Square root of the diffracted probe-beam intensity vs. time on different time scales after ps excitation of a dye-doped cholesteric liquid crystal at $t = 0$

1.4 Dye-doped cholesteric liquid crystals

Optically induced detuning of the selective reflectivity band in absorbing cholesteric liquid crystals has been succesfully used [38, 39] for intrinsic (mirror-less) optical bistability and optical switching. The dynamic response of dye doped cholesteric liquid crystals with an absorption maximum near the selective reflectivity band to a picosecond laser pulse in transient grating experiments [40] has been investigated recently to demonstrate that fast subnanosecond switching times can be achieved in such systems. Results are shown in Figs. 13 and 14. The film thickness has been about 2 μm, the excitation wavelength $\lambda_{exc} = 532$ nm was close to the absorption peak $\lambda_0 = 550$ nm and the peak reflectivity $\lambda_r = 570$ nm. Figure 13 displays a fast picosecond grating component, which has been recorded with a streak camera during self-diffraction experiments. In Fig. 14, time resolved grating relaxation shows that there are further contributions to the optical nonlinearity, which are caused by radiationless recombination of the excited molecules and

optical heating, resulting in density changes and molecular reorientation.

The fast ps grating component with diffraction efficiencies up to 10% into first diffraction order has been explained by a resonant optical nonlinearity due to saturation of the dye absorption. According to Kramers-Kronig relations [41] absorption saturation results also in refractive index changes which in cholesteric liquid crystals shift the selective reflectivity band. As a consequence, enhanced grating diffraction due to changes in the helical feedback can be obtained in these mesophases.

The absorbed intensity results also in a rapid increase in temperature, and the response to the corresponding thermal grating is exhibited in Fig. 14. The observed optical grating rise times are in the order of 200 to 400 ns and have been explained by thermally excited overdamped sound waves and density relaxations, very similar to the transient gratings in smectic A liquid crystals shown in the previous subsection.

The observed slower grating relaxation takes place on two different time scales mainly. Note that the end of the (lower) left curve in Fig. 14 is the beginning of the slower right curve. The faster component exhibits a nonexponential decay on a microsecond scale, whereas the slower relaxation can be fitted with a double exponential law using time constants of 30 and 270 ms, respectively. The microsecond decay is connected with surface heat diffusion out of the thin liquid crystal film and very similiar to the thermal grating relaxation observed in rather thin (2 μm) ferroelectric liquid crystals discussed above. The millisecond component is attributed to elastic helix deformations which relax by surface diffusion, since the sample is much thinner than the induced transversal grating period. Consequently, the double exponential decay and the corresponding two time constants can be appointed [10] to the first ($m=1$) and third ($m=3$) longitudinal Fourier components of the distortion. Since $\tau_m \sim (m\pi/d)^{-2}$ in this case, the observed relaxation times are expected to fulfill the relation $\tau_1 : \tau_3 = 9:1$ in good agreement with the experimental observations.

2 Conclusions

In the present paper we have reviewed fast transients of Kerr-like optical nonlinearities in various liquid crystals, which have been investigated with light-induced dynamic gratings using picosecond excitation pulses. It was shown that the use of short intense laser pulses with strong optical fields in connection with the transient grating technique may be a powerful tool for the investigation of different relaxation processes like molecular reorientation, fluctuations in temperature and density, ultrasound, flow and flow-alignment or phase transitions in these materials. The observed characteristic time constants and relaxation rates span up an enormeous time scale reaching from picoseconds for electronic effects like nonlinear absorption, up to several hundered milliseconds for the relaxation of elastic deformations and reorientation phenomena. In between, there are several nanosecond processes like acoustic gratings, density and order parameter relaxations, followed by thermal grating relaxation running on a microsecond scale.

In particular, the effects of optical reorientation, acoustic gratings and flow-alignment, but also electronic effects like nonlinear absorption have been observed and investigated in nematic liquid crystals. A new photothermally induced reorientation effect and polarization switching phenomena was investigated in thin surface stabilized ferroelectric SmC* liquid crystals. Fast saturation nonlinearities, in addition to subsequent thermal and elastic deformation gratings, have been further observed in dye-doped cholesteric liquid crystals. These experiments show, that the photonic response in liquid crystalline materials may be much faster if short intense laser pulses are used instead of low-power cw laser radiation. This may open up new aspects and perspectives in the research and application of optical nonlinear effects in liquid crystals. Although most of the investigations have been concentrated on the nematic phase up to now, the other mesophases look very promising as well, which was demonstrated with ferroelectric and cholesteric liquid crystals.

Acknowledgements. We like to thank B. Trösken and D. Grebe for collaboration and helpful discussions. The research programm has been supported by the Deutsche Forschungsgemeinschaft via the 'Sonderforschungsbereich' 315 "Anisotrope Fluide".

References

1. Y.R. Shen: *The Principles of Nonlinear Optics* (Wiley, New York 1984)
2. B.Y. Zel'dovich, N.V. Pilipetsky, V.V. Shkunov: *Principles of Phase Conjugation,* Springer Ser. Opt. Sci., Vol. 43 (Springer, Berlin, Heidelberg 1985)
3. P.W. Smith: Proc. SPIE **881**, 30 (1988)
4. R. Cunningham: Lasers Optronics **8**, 63 (1989)
5. I.C. Khoo, S.T. Wu: *Optics and Nonlinear Optics in Liquid Crystals* (World Scientific, Singapore 1993)
6. N.V. Tabiryan, A.V. Sukhov, B.Y. Zel'dovich: Mol. Cryst. Liq. Cryst. **136**, 1 (1986)
7. I.C. Khoo: Prog. Opt. **26**, 32 (North-Holland, Amsterdam 1988)
8. I. Janossy: In *Perspectives in Condensed Matter Physics;* ed. by L. Miglio (Kluwer, Dordrecht 1990)
9. P. Palffy-Muhoray: In *Liquid Crystals/Applications and Uses,* Vol. 1, ed. by B. Bahadur (World Scientific, Singapore 1990)
10. R. Macdonald, H.J. Eichler: In *Proc. 5th Topsøe Summer School on Nonlinear Optics,* ed. by O. Keller (Nova Science, New York) (to appear 1994)
11. H. Hsiung, L.P. Shi, Y.R. Shen: Phys. Rev. A **30**, 1453 (1984)
12. I.C. Khoo, R.G. Lindquist, R.R. Michael, R.J. Mansfield, P. LoPresti: J. Appl. Phys. **69**, 3853 (1991)
13. H.J. Eichler, R. Macdonald: Phys. Rev. Lett. **67**, 2666 (1991)
14. D. Armitage, S.M. Delwart: Mol. Cryst. Liq. Cryst. **122**, 59 (1985)
15. I.C. Khoo, R. Normandin: J. Appl. Phys. **55**, 1416 (1984)
16. I.C. Khoo, R. Normandin: Opt. Lett. **9**, 285 (1984)
17. H.J. Yuan, L. Li, P. Palffy-Muhoray: *Electro-optical Materials for Switches, Coatings, Sensor Optics and Detectors,* SPIE Proc. **1307** (1990)
18. H.J. Eichler, R. Macdonald: *Proc. Int'l Conf. Lasers '89,* ed. by D.G. Harris; T.M. Shay (STS, McLean 1990) p. 449
19. H.J. Eichler, R. Macdonald: Mol. Cryst. Liq. Cryst. **207**, 117 (1991)

20. H.J. Eichler, D. Günter, D.W. Pohl: *Laser-Induced Dynamic Gratings,* Springer Ser. Opt. Sci., Vol. 50 (Springer, Berlin, Heidelberg 1986)
21. H.J. Eichler, H. Stahl: J. Appl. Phys. **44**, 3429 (1973)
22. M.D. Fayer: IEEE J. QE–**22**, 1437 (1986)
23. W. Kaiser, M. Maier: In *Laser Handbook,* Vol. 2, ed. by F.T. Arecchi, E.O. Schulz-Dubois (North Holland, Amsterdam 1972) p. 1077
24. W.H. de Jeu: *Physical Properties of Liquid Crystals* (Gordon and Breach, London 1980)
G. Vertogen, W.H. de Jeu: *Thermotropic Liquid Crystals, Fundamentals,* Springer Ser. Chem. Phys., Vol. 45 (Springer, Berlin, Heidelberg 1988)
25. J.D. Jackson: *Classical Electrodynamics* (Wiley, New York 1975)
26. J.L. Ericksen, F.M. Leslie: Mol. Cryst. Liq. Cryst. **7**, 153 & 407 (1969)
27. S. Hess, I. Pardowitz: Z. Naturforsch. **36a**, 554 (1981)
28. J. Constant, E.P. Raynes: Mol. Cryst. Liq. Cryst. **62**, 115 (1980)
29. A.D. Lloyd, B.S. Wherrett: Appl. Phys. Lett. **53**, 460 (1988)
30. R. Macdonald, J. Schwartz, H.J. Eichler: Int. J. Nonlin. Opt. Phys. **1**, 103 (1992)
31. F.W. Deeg, M.D. Fayer: J. Chem. Phys. **91**, 2269 (1989)
32. H.J. Eichler, R. Macdonald, B. Trösken: Mol. Cryst. Liq. Cryst. **231**, 1 (1993)
33. C. David, D. Baeyens-Volant: Mol. Cryst. Liq. Cryst. **59**, 181 (1980)
34. R. Sander, R. Macdonald, R. Menzel, H.J. Eichler: J. Chem. Phys. Lett. (preprint)
35. R. Macdonald, D. Grebe: Phys. Rev. Lett. **70**, 2746 (1993)
36. R. Blinc, C. Filipic, A. Levstik, B. Zeks, T. Carlsson: Mol. Cryst. Liq. Cryst. **152**, 503 (1987)
37. D. Grebe, R. Macdonald: J. Phys. D **27**, 567 (1994)
38. L.I. Zagainova, G.V. Klimusheva, I.P. Kryzhanoskij, N.V. Kukhtarev: JETP Lett. **42**, 436 (1985)
39. R.B. Alaverdan, S.M. Arakelian, Y.S. Chilingarian: JETP Lett. **42**, 451 (1985)
40. H.J. Eichler, D. Grebe, R. Macdonald, A.G. Iljin, G.V. Klimusheva, L.I. Zagainova: Opt. Mater. **2**, 201 (1993)
41. A. Yariv: *Quantum Electronics* (Wiley, New York 1989)